Cardiac Magnetic Resonance Feature Tracking Myocardial Strain Analysis in Suspected Acute Myocarditis: Diagnostic Value and Association with Severity of Myocardial Injury

Qian Gao
First Affiliated Hospital of Kunming Medical University
Wenfang Yi
First Affiliated Hospital of Kunming Medical University
Chao Gao
First Affiliated Hospital of Kunming Medical University
Tianfu Qi
First Affiliated Hospital of Kunming Medical University
Lili Li
First Affiliated Hospital of Kunming Medical University
Kaipeng Xie
First Affiliated Hospital of Kunming Medical University
Wei Zhao
First Affiliated Hospital of Kunming Medical University
Wei Chen (chenwin2008@163.com)
First Affiliated Hospital of Kunming Medical University

Research Article

Keywords: Myocarditis, Cardiac magnetic resonance imaging, Feature tracking, Strain, Updated Lake Louise Criteria

Posted Date: July 28th, 2022

DOI: https://doi.org/10.21203/rs.3.rs-1878371/v1

Additional Declarations: No competing interests reported.

Version of Record: A version of this preprint was published at BMC Cardiovascular Disorders on March 28th, 2023. See the published version at https://doi.org/10.1186/s12872-023-03201-2.

Abstract

Background: Albeit that cardiac magnetic resonance feature tracking (CMR-FT) has enabled quantitative assessment of global myocardial strain in the diagnosis of suspected acute myocarditis, the cardiac segmental dysfunction remains understudied. The aim of the present study was using CMR-FT to assess the global and segmental dysfunction of the myocardium for diagnosis of suspected acute myocarditis.

Methods: 47 patients with suspected acute myocarditis (divided into impaired and preserved left ventricular ejection fraction [LVEF] groups) and 39 healthy controls (HCs) were studied. A total of 752 segments were divided into three subgroups, including segments with non-involvement (S_{Ni}), segments with edema (S_E), and segments with both edema and late gadolinium enhancement (S_{E+LGE}). 272 healthy segments served as the control group (S_{HCs}).

Results: Compared with HCs, patients with preserved LVEF showed impaired global circumferential strain (GCS) and global longitudinal strain (GLS). Segmental strain analysis showed that the peak radial strain (PRS), peak circumferential strain (PCS), and peak longitudinal strain (PLS) values significantly reduced in S_{E+LGE} compared with S_{HCs}, S_{Ni}, S_E. PCS significantly reduced in S_{Ni} (-15.3±5.8% vs. -20.3±6.4%, $p<0.001$) and S_E (-15.2±5.6% vs. -20.3±6.4%, $p<0.001$), compared with S_{HCs}. The area under the curve (AUC) values of GLS (0.723) and GCS (0.710) were higher than that of global peak radial strain (0.657) in the diagnosis of acute myocarditis. Model with updated Lake Louise Criteria could result in a further increase in diagnostic performance.

Conclusions: Global and segmental myocardial strain were impaired in patients with suspected acute myocarditis, even in the edema or relatively non-involved regions. CMR-FT may serve as an incremental tool for assessment of cardiac dysfunction and provide important additional imaging-evidence for distinguishing the different severity of myocardial injury in myocarditis.

Background

As an important cause of cardiac morbidity and mortality, myocarditis has been reported in up to 12% of young adults with sudden death (1, 2) and regarded as an important etiology underlying some other myocardial diseases (3). However, its diagnosis remains challenging and formidable due to its diversified clinical presentation. Endomyocardial biopsy, the current gold standard of myocarditis, is unsatisfactory due to its low sensitivity and specificity and invasiveness (4, 5). Cardiac magnetic resonance (CMR), combining morphological and functional imaging with myocardial tissue characterization, has enabled the detection of myocardial tissue characteristic of acute inflammation (e.g., cardiac dysfunction, myocardial edema, hyperemia, and necrosis), and is thus increasingly employed for diagnostic evaluation of patients with suspected acute myocarditis (6, 7). The current widely-accepted CMR-based criteria of myocarditis, the updated Lake Louise Criteria (LLC), relies on at least one T2-baesd criterion (increased myocardial T2-mapping or signal intensity in T2-weighted images) and one T1-based criterion (increased myocardial T1-mapping, extracellular volume(ECV), or late gadolinium enhancement(LGE))(8). In recent

years, a novel CMR approach called “feature tracking” (FT) (derived from CMR cine imaging) has allowed for quantitative assessment of global and segmental myocardial strain (9, 10) and helped the evaluation of cardiac dysfunction in early stages of both ischemic and non-ischemic cardiomyopathies. Albeit a few recent studies of the feasibility, sensitivity, and specificity of global myocardial strain parameters based on CMR-FT in the diagnosis of myocarditis (6, 9–12), there has been scant studies focusing on the segmental dysfunction of the myocardium by using CMR -FT. Recently, the 2D speckle tracking echocardiography (2D-STE) has been successfully employed to quantify myocardial deformations, which may be differentially manifested in suspected acute myocarditis (13). It is worth noting, nevertheless, the 2D-STE technique has some intrinsic limitations of its own. The most critical one lies in its temporal instability of tracking patterns (14). However, there has been a lack of CMR-FT studies related to edema or necrosis based on T2-weigehted and LGE images to quantitatively evaluate cardiac segmental dysfunction in suspected acute myocarditis. It remains to be clarified whether the severity of myocardial injury (e.g. edema, necrosis) is related to the regional myocardial dysfunction. Besides, it is also necessary to further probe into the diagnostic value of different strain parameters for patients with suspected acute myocarditis, especially in preserved LVEF. It is against this background of niches in this field that the present study has been carried out to look into the global and segmental dysfunction of the myocardium in suspected acute myocarditis and the diagnostic value of CMR-FT myocardial strain analysis. To be specific, this study investigated (1) whether FT-derived strain parameters can be used to differentiate patients with suspected acute myocarditis from healthy controls (HCs), (2) to what extent the changes in segmental strain parameters depend on the severity of myocardial injury in patients with suspected acute myocarditis, and (3) which myocardial strain parameters perform the best in detecting suspected acute myocarditis. We present the following article in accordance with the STARD reporting checklist.

Methods

Study population

This retrospective study was approved by the Institutional Review Boards of our hospital(No.2022-L-128). Forty-seven patients (35 males, 12 females) were retrospectively enrolled from 2015 to May 2019 in our hospital. All the patients had been clinically suspected acute myocarditis (mean symptom duration before referral: 5.2 ± 4.1 days, < 14 days for all the patients) and underwent CMR examination. They were diagnosed with myocarditis for having clinical symptoms and according to the corresponding clinical criteria based on 2013 ESC guidelines (15). Clinically suspected myocarditis refers to symptomatic patients (chest pain, dyspnea, palpitation, or other relevant cardiac symptoms) based on one or more diagnostic criteria (abnormal electrocardiography, elevated troponin, and functional or structural abnormalities confirmed by echocardiography or MR) and asymptomatic patients based on two or more of the above criteria. Coronary artery disease was ruled out prior to CMR in all patients (Table 1). The control group consisted of 39 age- and gender-matched healthy controls (HCs) (26 males, 13 females), who were selected for their uneventful medical histories, absence of symptoms indicative of

cardiovascular dysfunction, lack of abnormalities in electrocardiograms, echocardiography and CMR, and no history of inflammatory diseases.

Image acquisition

CMR was performed on a 3.0-T MR system (Achieva, Philips Healthcare, Best, Netherland) using a standard 16-element cardiac phased array coil and a four-lead vectorcardiogram. For functional analysis, electrocardiography-gated balance turbo field echo (b-TFE) cine images were obtained in the short-axis, four-chamber, and two-chamber views (TR, 3.2 ms; TE, 1.53 ms; FOV, 320 mm × 320mm; reconstruction matrix, 320 × 320; flip angle, 45°; slice thickness, 8 mm; space, 0 mm). Edema-sensitive black-blood T2-weighted images with fat saturation (triple inversion recovery turbo spin echo sequences with inversion pulses for fat and blood suppression) were acquired in the short-axis orientation covering the entire left ventricle (TR, 1200 ms; TE, 60 ms; FOV, 320 mm x 320 mm; reconstruction matrix, 352 × 352; slice thickness, 8 mm; space, 2 mm). Late gadolinium enhancement (LGE) imaging was performed 10 minutes after the injection of 0.1 mmol/kg gadobutrol (Gadovist, Bayer Healthcare, Leverkusen, Germany) with inversion time (300–340 mm) adjusted according to a Look-Locker inversion recovery-prepared T1-weighted phase-sensitive inversion recovery sequence (TR, 6.1 ms; TE, 3.0 ms; TI, 400 ms; FOV, 320 mm × 320 mm; reconstruction matrix, 320 × 320; flip angle, 25°; slice thickness, 8 mm; space, 2 mm) in the short-axis, four-chamber, and two-chamber views, which corresponded with cine images. CMR scanning was performed according to the standardized protocols recommended by the Society for Cardiovascular Magnetic Resonance (SCMR).(16)

Imaging analysis

Three radiologists experienced in CMR diagnosis blindly analyzed the data, performed the measurements, and reached agreement regarding the consequences.

Cardiac function analysis

Cardiac function analysis was performed offline based on the acquired b-TFE cine images by using dedicated software (CVI 42 v. 5.6, Circle Cardiovascular Imaging Inc., Calgary, AB, Canada). Endocardial and epicardial contours of the left ventricle were manually delineated at the end-systolic and end-diastolic phases using a three-dimensional short tool to calculate volume changes and left ventricular ejection fraction (LVEF). Based upon the body surface area, LV end-diastolic volume index, LV end-systolic volume index, and myocardial mass index were quantified. Patients with acute myocarditis were divided into two subgroups according to LVEF, including the impaired-LVEF group (LVEF < 55%; n = 12) and the preserved-LVEF group (LVEF ≥ 55%; n = 35) (9).

The updated LLC

Image analysis of the updated LLC was performed using the CVI 42 software (CVI 42 v. 5.6, Circle Cardiovascular Imaging Inc., Calgary, AB, Canada). The myocardium was divided into 16 segments according to the American Heart Association segmentation (17). Every segment was evaluated for the following tissue characterizations: 1) T2-based marker for myocardial edema with either T2-weighted

imaging or T2 mapping, and 2) T1-based marker for associated myocardial injury: one of the three methods, namely, LGE, T1-mapping or extracellular volume (ECV).

CMR diagnosis of myocarditis was based on the edema-sensitive CMR (T2-weighted images or T2 mapping) and at least one additional T1-based tissue characterization technique (8). As T1 and T2 mapping and ECV are not routine sequences in our institution, the approach chosen by our study included only T2-weighted imaging and LGE. T2-weighted imaging is identified visually on T2-weighted black-blood imaging and by calculating the T2 ratio of ≥ 1.9 (signal intensity normalized to skeletal muscle in the same slice) (8, 18). The patterns of LGE are commonly and typically located in the subepicardial and midmyocardial regions (8). All the myocardial segments of the enrolled patients were divided into three subgroups based on the severity of their myocardial injury (19), viz. segments with non-involvement (S_{Ni}; n = 509), segments with edema (S_E; n = 89), and segments with both edema and LGE (S_{E+LGE}; n = 154). The S_E subgroup was localized using T2-weighted images; the S_{E+LGE} subgroup was localized using both T2-weighted images and LGE images; and the S_{Ni} subgroup was considered as normal in comparison with the two preceding subgroups. A cohort of segments of HCs (S_{HCs}; n = 272) served as the control group.

Myocardial strain analysis using CMR-FT

CMR-FT was performed offline based on the acquired b-TFE cine images using CVI 42 software (CVI 42 v. 5.6, Circle Cardiovascular Imaging Inc., Calgary, AB, Canada). Endocardial and epicardial contours were drawn manually in the end-diastolic phases, and myocardial strain was automatically tracked by CVI 42 throughout the cardiac cycle. Global peak longitudinal strain (GLS) was averaged from the measurements of the two-, three-, and four-chamber views. Circumferential (GCS) and radial (GRS) peak strain parameters were determined in the short-axis view covering the entire left ventricle (Fig. 1). Every segment was evaluated for myocardial strain parameters to obtain segmental peak radial strain (PRS), peak circumferential strain (PCS), and peak longitudinal strain (PLS).

Statistical analysis

Normality was tested with the Kolmogorov-Smirnov test. Continuous variables were presented as means ± standard deviations and compared using the Student's t-test for normally distributed data or the Mann-Whitney U-test for non-normally distributed data. Parametric data of more than two groups were compared using one-way analysis of variance testing. Post-hoc testing was performed with the least significant difference test (homogeneity of variance) or Dunnett's T3 test (heterogeneity of variance). Categorical group data presented as percentages were compared using the chi-squared test or Fisher's exact test, as appropriate. Diagnostic performance of the strain parameters was analyzed by plotting receiver operating characteristic curves and comparing the areas under those curves. Cutoff values were chosen by maximizing reclassification accuracy for the predictive variables, and reclassification sensitivity, specificity, and accuracy were calculated. To combine the single predictive variables, scores

were derived from logistic regression analysis. The level of statistical significance was set to $p < 0.050$. Statistical analysis was performed using SPSS software(v.25.0, IBM SPSS Statistics, Armonk, NY, USA).

Results

Population characteristics

This study included forty-seven patients with suspected acute myocarditis and 39 HCs. Clinical symptoms of the patients are given in Table 1. Demographic characteristics of the HCs and the patients, LV volumetric parameters, and updated LLC data are presented in Table 2.

Table 1
Classification of Patients with Suspected Acute Myocarditis According to Clinical Criteria(15)

	Myocarditis patients(n = 47)
Clinical symptoms consistent with myocarditis	
Acute chest pain	40
New-onset(days up to 3 months) or worsening of: dyspnea at rest or exercise/fatigue, with or without left and/or right heart failure signs	15
Palpitations /arrhythmia symptoms /syncope/ aborted sudden cardiac death	8
Cardiogenic shock	1
Diagnostic criteria consistent with myocarditis	
ECG / Holter / stress test features	42
Elevated TnT/TnI	29
Functional and structural abnormalities on cardiac imaging (echo/angio/CMR)	12
Exclusion of coronary artery disease (CAD)	
Cardiac catheterization	17
Cardiac computed tomography angiography	30

Table 2
Characteristics of Patients with Suspected Acute Myocarditis (Subgroups with Preserved and Impaired Left Ventricular Ejection Fraction) and Controls

Parameter	Controls(N = 39)	Myocarditis(N = 47)	Myocarditis with preserved LVEF(N = 35)	Myocarditis with impaired LVEF(N = 12)
female/male	13/26	12/35	7/28	5/7
Age(years)	33 ± 12	31 ± 13	30 ± 14	32 ± 11
Height(cm)	166 ± 8	167 ± 8	168 ± 9	166 ± 8
Weight(kg)	60 ± 13	63 ± 12	63 ± 14	61 ± 8
Heart rate(bpm)	74 ± 14	74 ± 15	75 ± 17	72 ± 8
BSA(ml/m^2)	1.64 ± 0.21	1.67 ± 0.20	1.68 ± 0.20	1.64 ± 0.14
Symptom duration before CMR (days)	n.a	5.2 ± 4.1	5.0 ± 3.8	5.5 ± 4.7
Initial TnT(ng/ml, NR: 0.006)	n.a	11.1 ± 13.6	10.6 ± 15.1	12.1 ± 10
Initial MYO(µg/L, NR: 110)	n.a	275 ± 298	241 ± 306	279 ± 235
Initial CK-MB(ng/ml, NR: 24.0)	n.a	19.7 ± 20.9	15.6 ± 16.5[c]	33.4 ± 24.5[b]
Initial CRP(mg/L, NR: 6.0)	n.a	60.8 ± 95.7	95.3 ± 110.3[c]	5.6 ± 3.3[b]
LVED volume/BSA(ml/m^2)	71.6 ± 12.1	80.7 ± 31.2	74.1 ± 16.7[c]	89.6 ± 26.2[ab]
LVES volume/BSA(ml/m^2)	22.7 ± 6	34.7 ± 26[#]	25.6 ± 7.6[c]	54.9 ± 24.2[ab]
LV ejection fraction(%)	68.3 ± 6.2	59.4 ± 14.3[#]	65.5 ± 5.9[c]	40.0 ± 14.8[ab]
LVED wall mass/BSA(g/m^2) (without papillary muscles)	49.8 ± 12.6	58.1 ± 13.4[#]	54.9 ± 10.1[c]	66.2 ± 17.6[ab]
T2 Ratio	1.8 ± 0.2	2.3 ± 0.6[#]	2.2 ± 0.4[a]	2.5 ± 0.9[a]
2 out of 2 updated LLC(%)	0	72.3	68.6	83.3

BSA, body surface area; ED, end diastolic; ES, end systolic; LV, left ventricle; LLC, Lake Louise Criteria; NR, normal range

[#, a] Significant difference compared to controls

[b] Significant difference compared to patients with preserved left ventricular ejection fraction

[c] Significant difference compared to patients with impaired left ventricular ejection fraction

Parameter	Controls(N = 39)	Myocarditis(N = 47)	Myocarditis with preserved LVEF(N = 35)	Myocarditis with impaired LVEF(N = 12)
1 out of 2 updated LLC(%)	28.2	17.1	17.1	16.7
0 out of 2 updated LLC(%)	71.8	10.6	14.3	0
BSA, body surface area; ED, end diastolic; ES, end systolic; LV, left ventricle; LLC, Lake Louise Criteria; NR, normal range				
[#, a] Significant difference compared to controls				
[b] Significant difference compared to patients with preserved left ventricular ejection fraction				
[c] Significant difference compared to patients with impaired left ventricular ejection fraction				

Global strain analysis between patients and HCs

Compared with HCs, patients with suspected acute myocarditis showed significantly impaired GRS (32.5 ± 12.0% vs. 40.8 ± 10.8%; $p = 0.001$), GCS (-14.6 ± 3.7%-vs. 17.4 ± 2.8% ; $p < 0.001$), and GLS (-12.2 ± 2.5% vs. -14.5 ± 2.5%; $p < 0.001$) (Fig. 2a-c). Patients with impaired LVEF showed significantly decreased GRS (21.2 ± 10.3%vs. 40.8 ± 10.8%; $p < 0.001$), GCS (-11.0 ± 3.8%vs. -17.4 ± 2.8% ; $p < 0.001$), and GLS (-9.6 ± 2.7% vs. -14.5 ± 2.5%; $p < 0.001$) as compared with HCs (Fig. 2a-c). Patients with preserved LVEF also showed significantly decreased GCS (-15.9 ± 2.8%vs. -17.4 ± 2.8%; $p = 0.029$) and GLS (-13.0 ± 1.8%vs. -14.5 ± 2.5%; $p = 0.007$) as compared with HCs, whereas their GRS values were not significantly different from that of the HCs(36.3 ± 10.1%vs. 40.8 ± 10.8%; $p = 0.072$). The three global strain parameters significantly decreased in patients with impaired-LVEF as compared with that in the preserved-LVEF group ($p < 0.010$) (Fig. 2d-f).

Segmental strain analysis in patients with suspected myocarditis based on severity of myocardial injury

PRS, PCS, and PLS values significantly reduced in S_{E+LGE} as compared with that in S_{HCs}, S_{Ni} and S_E groups. PCS significantly reduced in S_{Ni} (-15.3 ± 5.8% vs. -20.3 ± 6.4%, $p < 0.001$) and S_E (-15.2 ± 5.6% vs. -20.3 ± 6.4%, $p < 0.001$) groups as compared with that in S_{HCs} group. However, S_{Ni} and S_E groups were not significantly different from each other in their PRS, PCS, and PLS (Fig. 2g-i). All CMR segmental strain parameters for each subgroup evaluated are given in Table 3.

Table 3
Segmental strain values of three patient groups and healthy controls.

	Healthy Controls(n = 272)	Non-involvement segments(n = 509)	Edema segments(n = 89)	Edema + LGE segments(n = 154)
Peak Radial Strain[%]	36.7 ± 16.1[d]	37.3 ± 23.6[d]	38.5 ± 25.4[d]	28.1 ± 24.3[abc]
Peak Circumferential Strain[%]	-20.3 ± 6.4[bcd]	-15.3 ± 5.8[ad]	-15.2 ± 5.6[ad]	-13.0 ± 7.2[abc]
Peak Longitudinal Strain[%]	-13.4 ± 3.7[d]	-12.8 ± 7.6[d]	-12.6 ± 5.6[d]	-10.8 ± 7.3[abc]
[#, a] Significant difference compared to healthy controls				
[b] Significant difference compared to non-involvement segments				
[c] Significant difference compared to edema segments				
[d] Significant difference compared to edema + LGE segments				

Diagnostic performance of strain indices and strain parameters in patients with preserved ejection fraction

GLS and GCS showed good performance in the diagnosis of suspected acute myocarditis, with area under the curve (AUC) being 0.723 and 0.710, respectively. The diagnostic performance of GRS had an AUC of 0.657 (Fig. 3a). The optimal cutoff values of GRS, GCS, and GLS were 33.08%, -17.07%, and −12.77%, respectively. The updated LLC yielded excellent diagnostic performance (AUC: 0.894). However, the diagnostic performance of the combined scores of GCS, GLS, and GRS with updated LLC were further improved (AUC: 0.935, 0.928, and 0.919, respectively) (Fig. 3b). Sensitivities, specificities, accuracies, positive predictive values, and negative predictive values for all parameters are given in Table 4.

Table 4
Diagnostic Performance of Different Cardiac Magnetic Resonance Strain Parameters for Diagnosis of Suspected Acute Myocarditis

	AUC	Sensitivity[%]	Specificity[%]	Accuracy[%]	PPV[%]	NPV[%]
Global Peak Radial Strain	0.657	53	79	65	75	58
Global Peak Circumferential Strain	0.710	74	56	66	67	64
Global Peak Longitudinal Strain	0.723	60	74	66	74	60
Combinations						
Updated LLC	0.894	72	100	85	100	75
Updated LLC + Global Peak Radial Strain	0.919	77	100	87	100	87
Updated LLC + Global Peak Circumferential Strain	0.935	85	90	87	91	83
Updated LLC + Global Peak Longitudinal Strain	0.928	79	97	87	97	79

Discussion

We retrospectively investigated the global and segmental dysfunction of the myocardium and diagnostic value of CMR-FT myocardial strain analysis in suspected acute myocarditis. The major findings of this study are as follows: firstly, cardiac deformations measured by CMR-FT were significantly impaired in patients with suspected acute myocarditis and even in those with preserved LVEF; secondly, compared with global analysis, analysis of segmental myocardial strain made it possible to distinguish myocardial injuries in more detail. PRS, PLS and PCS were significantly impaired in the edema and LGE/necrosis segments. PCS significantly reduced in the LGE negative (edema or non-involvement segments) myocardium in suspected acute myocarditis. Lastly, GLS and GCS derived from CMR-FT showed good performance in diagnosis of patients with suspected acute myocarditis.

Differences in myocardial strain parameters

Strain parameters like GLS and GCS considerably reduced in patients with suspected acute myocarditis and even in those with preserved LVEF as compared with that in HCs. However, there was no difference in GRS between patients with preserved LVEF and HCs, which is in agreement with the results of previous

CMR and echocardiographic studies (9–12, 20–22). Overall, these results suggest that myocardial strain parameters, esp. longitudinal and circumferential strain parameters, can detect even subtle alterations in myocardial function (11, 12). There are probably two reasons for this. Firstly, the myocardium of the left ventricle typically consists of three myocardial layers, including the inner oblique, the middle circular, and the outer oblique. Fibers on the middle and outer myocardial layers produce both circumferential and longitudinal deformation during systole (23, 24). However, the radial deformation is determined by the three layers of the myocardium. Edema and necrotic inflammatory changes in acute myocarditis most commonly affect the epicardial layer of the myocardium. During systole, the inner oblique layer undergoes the biggest dimensional changes whereas functional alterations predominantly occur only when the endocardial layer is involved (25). Therefore, circumferential and longitudinal function might be affected early even if LVEF is preserved. In comparison, radial function might be less affected in myocarditis, which mostly does not affect the endocardium. Radial function might be damaged when ejection fraction is impaired, which may indicate that the endocardial layer is affected. Secondly, previous CMR-FT studies reported that global radial strain showed considerably lower intra- and inter-observer reproducibility as compared with longitudinal and circumferential strain. Some researchers (26, 27) proposed that this may be related to the measurement of an interaction between the endocardial border and the myocardial border during CMR feature tracking, which is not necessary for the derivation of longitudinal and circumferential strain parameters. As the distance between the endocardium and the epicardium is small, there may be systolic elimination of visible blood spaces between trabeculae that exaggerate the apparent shift of the endocardial boundary. To be brief, CMR-FT can detect cardiac systolic dysfunction of myocarditis earlier than the traditional ejection fraction, and GLS and GCS can be effective indicators for early detection of cardiac dysfunction of myocarditis.

Severity of myocardial injury and segmental myocardial strain parameters

As it is known that different myocardial segments are not equally affected by inflammatory processes in acute myocarditis. Histopathological features of acute myocarditis include cellular infiltration, edema, necrosis, and fibrotic scars (28, 29). Compared to global analysis, segmental myocardial strain analysis makes it possible to distinguish the myocardial injury in more detail. Recently, Chen et al.(30) has found that even the values of GRS, GCS and GLS were significantly lower in the LGE negative (with or without edema) group than that in the control group. Impairment of the myocardial strain was more severe in patients with LGE positive myocarditis. Ravesh et al. (31) found that the segmental myocardial strain (longitudinal, radial, and circumferential) made it possible to differentiate patient groups with different EF values, and they also found that the circumferential deformation analysis was more sensitive for patients with inconspicuous EF values. However, these studies did not make clear the relationship between segmental myocardial strain changes and myocardial injury. The current study found that segmental PLS, PCS, and PRS values were markedly impaired in the edema and LGE positive segments, thus indicating that myocardial injury is more severe in the presence of LGE. These findings are consistent with that by previous investigations (30, 32). Strikingly, even reduced PCS values in edema–only and non-involved segments can be detected as compared with healthy control segments. However, PLS and PRS

values of non-involved, edema and healthy segments only marginally changed. This study helps confirm the proposition that the edema, or even relatively normal myocardium, suffers from significant contractile impairment early after myocarditis. These phenomena may be ascribed to three causes. Firstly, histopathological analysis suggested that the myocardial edema reduces its contractility by enlarging the distance between actin and myosin filaments (33). Secondly, unlike myocardial infarction which is typically related to coronary artery supply territories (34), the non-involvement and edema segments are patchily distributed in myocarditis (35), suggesting that the non-involvement segments may be impacted by the adjacent edema region, which may explain the reduced contractility of the non-involvement segments. Lastly, the circumferential strain may be the most sensitive parameter for regional deformation as compared with longitudinal and radial deformation.

In recent years, given the highly variable natural history and prognosis of myocarditis (ranging from complete recovery to severe cardiomyopathy or sudden death), there is great interest in techniques for predicting the risk of future adverse outcomes. LGE and abnormalities of GLS have been shown to be powerful predictors of adverse events in myocarditis (21, 29, 36–39). Meanwhile, in previous studies, improvement in regional contractile function was found after the regression of edema in acute myocardial infarction (34). This study finds the LGE negative segments have preserved longitudinal strain in acute myocarditis, suggesting that the LGE negative myocardium may have a lower incidence of adverse events, and thus may recover after edema regression. This finding may provide new evidence for risk stratification of myocarditis, which may help improve patient care (40), and shed some light on the mechanism underlying the prognostic value of myocardial edema imaging.

Diagnostic performance of FT-derived strain indices

The current CMR criteria (updated LLC) for diagnosis of myocarditis use tissue characteristics. The evaluation of cardiac function has only supportive character in the updated LLC. However, as many myocarditis patients show impaired cardiac strains despite their preserved LVEF, the assessment of cardiac deformation has a potential to tap for improving diagnosis of myocarditis of these patients. The current study was intended to investigate the diagnostic performance of strain parameters of the preserved-LVEF group. Although GLS and GCS showed moderate diagnostic potential (AUC: 0.723 and 0.71, respectively) for suspected acute myocarditis, they also revealed a considerable overlap between HCs and patients with suspected myocarditis. GRS presented a slightly lower diagnostic performance (AUC: 0.693), which supports previous studies(11, 12). We focused only on suspected myocarditis patients with preserved LVEF, hoping that we might help explain the lower diagnostic performance of strain parameters as compared with a recent study by Luetkens et al (6), who demonstrated a considerably better diagnostic performance of GLS alone (AUC: 0.83), possibly because patients in their study were not divided into subgroups based on whether LVEF was preserved or not. In our study, the updated LLC still exhibited a high diagnostic potential (AUC: 0.893). The combination of updated LLC with strain parameters may outperform the updated LLC in our study. Thus, we suggest that GCS and GLS may serve as novel parameters for detecting myocardial dysfunction in patients with suspected

acute myocarditis and even in those with preserved LVEF. Therefore, strain assessment may have some incremental diagnostic advantages over traditional CMR imaging features.

Limitations

The present study has several limitations of its own. Firstly, we used a clinical reference standard for suspected myocarditis patients as subjects without endomyocardial biopsy. However, we carefully defined the patient cohort based on clinical criteria similar to that of other studies (6, 7). Nevertheless, some patients, in whom a differential cause of disease might have been missed, may possibly have some confounding effect on our cohort. Secondly, the number of patients was relatively small, which may affect the generalization of the research. Therefore, in future larger and prospective studies, sub-analyses should be performed with respect to different presentation types to determine the additional value of strain analysis in different clinical scenarios. Despite that CMR offers the possibility of advanced tissue characterization by using mapping technique (11, 12), the assessment of these techniques was beyond the scope of this study. Thus, further investigation by combining cardiac strain analysis with tissue mapping techniques is needed for future research.

Conclusions

Global and segmental myocardial strain were impaired in patients with suspected acute myocarditis, even in the edema or relatively non-involved regions. CMR-FT may serve as an incremental tool for assessment of cardiac dysfunction and provide important additional imaging-evidence for distinguishing the different severity of myocardial injury in myocarditis.

Declarations

Ethics approval and consent to participate: The authors are accountable for all aspects of the work in ensuring that questions related to the accuracy or integrity of any part of the work are appropriately investigated and resolved. The study was conducted in accordance with the Declaration of Helsinki (as revised in 2013). All methods were carried out in accordance with relevant guidelines and regulations. Informed consent was obtained from all subjects. The study was approved by Institutional Review Boards of the 1st Affiliated Hospital of Kunming Medical University (No.2022-L-128).

Consent for publication: Not applicable

Availability of data and materials: The datasets used and analysed during the current study are available from the corresponding author on reasonable request.

Competing Interests: The authors declare that they have no competing interests

Funding: This work was supported by the National Natural Science Foundation of China [No.:82060312]; and the Yunnan Applied Basic Research Projects [No.2018FE001(-039)].

Authors' contributions:

- Conceptualization and design: Qian Gao, Wei Chen
- Administrative support: Wei Zhao, Wei Chen
- Provision of study materials or patients: Chao Gao, Tianfu Qi, Lili Li, Kaipeng Xie, Wei Chen
- Collection and assembly of data: Qian Gao, Wenfang Yi, Wei Chen
- Data analysis and interpretation: Qian Gao, Wei Chen
- Manuscript writing: Qian Gao, Wenfang Yi, Chao Gao, Tianfu Qi, Lili Li, Kaipeng Xie, Wei Zhao, Wei Chen
- Final approval of manuscript: Qian Gao, Wenfang Yi, Chao Gao, Tianfu Qi, Lili Li, Kaipeng Xie, Wei Zhao, Wei Chen

Acknowledgements: Not applicable

References

1. Fabre A, Sheppard MN. Sudden adult death syndrome and other non-ischaemic causes of sudden cardiac death. Heart 2006;92:316–20.
2. Puranik R, Chow CK, Duflou JA, Kilborn MJ, McGuire MA. Sudden death in the young. Heart Rhythm 2005;2:1277–82.
3. Calabrese F, Basso C, Carturan E, Valente M, Thiene G. Arrhythmogenic right ventricular cardiomyopathy/dysplasia: is there a role for viruses? Cardiovasc Pathol 2006;15:11–7.
4. Biesbroek PS, Beek AM, Germans T, Niessen HW, van Rossum AC. Diagnosis of myocarditis: Current state and future perspectives. Int J Cardiol 2015;191:211–9.
5. Cooper LT, Jr., Fairweather D. We see only what we look for: imaging cardiac inflammation. Circ Cardiovasc Imaging 2013;6:165–6.
6. Luetkens JA, Homsi R, Sprinkart AM, Doerner J, Dabir D, Kuetting DL, Block W, Andrié R, Stehning C, Fimmers R, Gieseke J, Thomas DK, Schild HH, Naehle CP. Incremental value of quantitative CMR including parametric mapping for the diagnosis of acute myocarditis. Eur Heart J Cardiovasc Imaging 2016;17:154–61.
7. Luetkens JA, Doerner J, Thomas DK, Dabir D, Gieseke J, Sprinkart AM, Fimmers R, Stehning C, Homsi R, Schwab JO, Schild H, Naehle CP. Acute myocarditis: multiparametric cardiac MR imaging. Radiology 2014;273:383–92.
8. Ferreira VM, Schulz-Menger J, Holmvang G, Kramer CM, Carbone I, Sechtem U, Kindermann I, Gutberlet M, Cooper LT, Liu P, Friedrich MG. Cardiovascular Magnetic Resonance in Nonischemic Myocardial Inflammation: Expert Recommendations. J Am Coll Cardiol 2018;72:3158–76.
9. Baeßler B, Schaarschmidt F, Dick A, Michels G, Maintz D, Bunck AC. Diagnostic implications of magnetic resonance feature tracking derived myocardial strain parameters in acute myocarditis. Eur

J Radiol 2016;85:218–27.

10. André F, Stock FT, Riffel J, Giannitsis E, Steen H, Scharhag J, Katus HA, Buss SJ. Incremental value of cardiac deformation analysis in acute myocarditis: a cardiovascular magnetic resonance imaging study. Int J Cardiovasc Imaging 2016;32:1093–101.
11. Baeßler B, Treutlein M, Schaarschmidt F, Stehning C, Schnackenburg B, Michels G, Maintz D, Bunck AC. A novel multiparametric imaging approach to acute myocarditis using T2-mapping and CMR feature tracking. J Cardiovasc Magn Reson 2017;19:71.
12. Luetkens JA, Schlesinger-Irsch U, Kuetting DL, Dabir D, Homsi R, Doerner J, Schmeel FC, Fimmers R, Sprinkart AM, Naehle CP, Schild HH, Thomas D. Feature-tracking myocardial strain analysis in acute myocarditis: diagnostic value and association with myocardial oedema. Eur Radiol 2017;27:4661–71.
13. Meindl C, Paulus M, Poschenrieder F, Zeman F, Maier LS, Debl K. Patients with acute myocarditis and preserved systolic left ventricular function: comparison of global and regional longitudinal strain imaging by echocardiography with quantification of late gadolinium enhancement by CMR. Clin Res Cardiol 2021;110:1792–800.
14. Voigt JU, Pedrizzetti G, Lysyansky P, Marwick TH, Houle H, Baumann R, Pedri S, Ito Y, Abe Y, Metz S, Song JH, Hamilton J, Sengupta PP, Kolias TJ, d'Hooge J, Aurigemma GP, Thomas JD, Badano LP. Definitions for a common standard for 2D speckle tracking echocardiography: consensus document of the EACVI/ASE/Industry Task Force to standardize deformation imaging. J Am Soc Echocardiogr 2015;28:183–93.
15. Caforio AL, Pankuweit S, Arbustini E, Basso C, Gimeno-Blanes J, Felix SB, Fu M, Heliö T, Heymans S, Jahns R, Klingel K, Linhart A, Maisch B, McKenna W, Mogensen J, Pinto YM, Ristic A, Schultheiss HP, Seggewiss H, Tavazzi L, Thiene G, Yilmaz A, Charron P, Elliott PM. Current state of knowledge on aetiology, diagnosis, management, and therapy of myocarditis: a position statement of the European Society of Cardiology Working Group on Myocardial and Pericardial Diseases. Eur Heart J 2013;34:2636-48, 48a-48d.
16. Kramer CM, Barkhausen J, Bucciarelli-Ducci C, Flamm SD, Kim RJ, Nagel E. Standardized cardiovascular magnetic resonance imaging (CMR) protocols: 2020 update. J Cardiovasc Magn Reson 2020;22:17.
17. Cerqueira MD, Weissman NJ, Dilsizian V, Jacobs AK, Kaul S, Laskey WK, Pennell DJ, Rumberger JA, Ryan T, Verani MS. Standardized myocardial segmentation and nomenclature for tomographic imaging of the heart. A statement for healthcare professionals from the Cardiac Imaging Committee of the Council on Clinical Cardiology of the American Heart Association. Circulation 2002;105:539–42.
18. Abdel-Aty H, Boyé P, Zagrosek A, Wassmuth R, Kumar A, Messroghli D, Bock P, Dietz R, Friedrich MG, Schulz-Menger J. Diagnostic performance of cardiovascular magnetic resonance in patients with suspected acute myocarditis: comparison of different approaches. J Am Coll Cardiol 2005;45:1815–22.

19. Korkusuz H, Esters P, Naguib N, Nour Eldin NE, Lindemayr S, Huebner F, Koujan A, Bug R, Ackermann H, Vogl TJ. Acute myocarditis in a rat model: late gadolinium enhancement with histopathological correlation. Eur Radiol 2009;19:2672–8.
20. Weigand J, Nielsen JC, Sengupta PP, Sanz J, Srivastava S, Uppu S. Feature Tracking-Derived Peak Systolic Strain Compared to Late Gadolinium Enhancement in Troponin-Positive Myocarditis: A Case-Control Study. Pediatr Cardiol 2016;37:696–703.
21. Hsiao JF, Koshino Y, Bonnichsen CR, Yu Y, Miller FA, Jr., Pellikka PA, Cooper LT, Jr., Villarraga HR. Speckle tracking echocardiography in acute myocarditis. Int J Cardiovasc Imaging 2013;29:275–84.
22. Uppu SC, Shah A, Weigand J, Nielsen JC, Ko HH, Parness IA, Srivastava S. Two-dimensional speckle-tracking-derived segmental peak systolic longitudinal strain identifies regional myocardial involvement in patients with myocarditis and normal global left ventricular systolic function. Pediatr Cardiol 2015;36:950–9.
23. Sengupta PP, Tajik AJ, Chandrasekaran K, Khandheria BK. Twist mechanics of the left ventricle: principles and application. JACC Cardiovasc Imaging 2008;1:366–76.
24. Ho SY. Anatomy and myoarchitecture of the left ventricular wall in normal and in disease. Eur J Echocardiogr 2009;10:iii3-7.
25. Sarvari SI, Haugaa KH, Zahid W, Bendz B, Aakhus S, Aaberge L, Edvardsen T. Layer-specific quantification of myocardial deformation by strain echocardiography may reveal significant CAD in patients with non-ST-segment elevation acute coronary syndrome. JACC Cardiovasc Imaging 2013;6:535–44.
26. Schmidt B, Dick A, Treutlein M, Schiller P, Bunck AC, Maintz D, Baeßler B. Intra- and inter-observer reproducibility of global and regional magnetic resonance feature tracking derived strain parameters of the left and right ventricle. Eur J Radiol 2017;89:97–105.
27. Pedrizzetti G, Claus P, Kilner PJ, Nagel E. Principles of cardiovascular magnetic resonance feature tracking and echocardiographic speckle tracking for informed clinical use. J Cardiovasc Magn Reson 2016;18:51.
28. Mahrholdt H, Wagner A, Deluigi CC, Kispert E, Hager S, Meinhardt G, Vogelsberg H, Fritz P, Dippon J, Bock CT, Klingel K, Kandolf R, Sechtem U. Presentation, patterns of myocardial damage, and clinical course of viral myocarditis. Circulation 2006;114:1581–90.
29. Grün S, Schumm J, Greulich S, Wagner A, Schneider S, Bruder O, Kispert EM, Hill S, Ong P, Klingel K, Kandolf R, Sechtem U, Mahrholdt H. Long-term follow-up of biopsy-proven viral myocarditis: predictors of mortality and incomplete recovery. J Am Coll Cardiol 2012;59:1604–15.
30. Chen Y, Sun Z, Xu L, Liu J, Li Y, Zhang N, Liu D, Wen Z. Diagnostic and Prognostic Value of Cardiac Magnetic Resonance Strain in Suspected Myocarditis With Preserved LV-EF: A Comparison Between Patients With Negative and Positive Late Gadolinium Enhancement Findings. J Magn Reson Imaging 2021.
31. Salehi Ravesh M, Eden M, Langguth P, Piesch TC, Lehmann JK, Lebenatus A, Hauttemann D, Graessner J, Frey N, Jansen O, Both M. Non-contrast enhanced diagnosis of acute myocarditis based

on the 17-segment heart model using 2D-feature tracking magnetic resonance imaging. Magn Reson Imaging 2020;65:155–65.

32. Zhu J, Chen Y, Xu Z, Wang S, Wang L, Liu X, Gao F. Non-invasive assessment of early and acute myocarditis in a rat model using cardiac magnetic resonance tissue tracking analysis of myocardial strain. Quant Imaging Med Surg 2020;10:2157–67.
33. Ruzsics B, Surányi P, Kiss P, Brott BC, Litovsky S, Denney TS, Jr., Aban I, Lloyd SG, Simor T, Elgavish GA, Gupta H. Myocardial strain in sub-acute peri-infarct myocardium. Int J Cardiovasc Imaging 2009;25:151–9.
34. Kidambi A, Mather AN, Swoboda P, Motwani M, Fairbairn TA, Greenwood JP, Plein S. Relationship between myocardial edema and regional myocardial function after reperfused acute myocardial infarction: an MR imaging study. Radiology 2013;267:701–8.
35. Korkusuz H, Esters P, Huebner F, Bug R, Ackermann H, Vogl TJ. Accuracy of cardiovascular magnetic resonance in myocarditis: comparison of MR and histological findings in an animal model. J Cardiovasc Magn Reson 2010;12:49.
36. Gräni C, Eichhorn C, Bière L, Murthy VL, Agarwal V, Kaneko K, Cuddy S, Aghayev A, Steigner M, Blankstein R, Jerosch-Herold M, Kwong RY. Prognostic Value of Cardiac Magnetic Resonance Tissue Characterization in Risk Stratifying Patients With Suspected Myocarditis. J Am Coll Cardiol 2017;70:1964–76.
37. Aquaro GD, Perfetti M, Camastra G, Monti L, Dellegrottaglie S, Moro C, Pepe A, Todiere G, Lanzillo C, Scatteia A, Di Roma M, Pontone G, Perazzolo Marra M, Barison A, Di Bella G. Cardiac MR With Late Gadolinium Enhancement in Acute Myocarditis With Preserved Systolic Function: ITAMY Study. J Am Coll Cardiol 2017;70:1977–87.
38. Lee JW, Jeong YJ, Lee G, Lee NK, Lee HW, Kim JY, Choi BS, Choo KS. Predictive Value of Cardiac Magnetic Resonance Imaging-Derived Myocardial Strain for Poor Outcomes in Patients with Acute Myocarditis. Korean J Radiol 2017;18:643–54.
39. Awadalla M, Mahmood SS, Groarke JD, Hassan MZO, Nohria A, Rokicki A, Murphy SP, Mercaldo ND, Zhang L, Zlotoff DA, Reynolds KL, Alvi RM, Banerji D, Liu S, Heinzerling LM, Jones-O'Connor M, Bakar RB, Cohen JV, Kirchberger MC, Sullivan RJ, Gupta D, Mulligan CP, Shah SP, Ganatra S, Rizvi MA, Sahni G, Tocchetti CG, Lawrence DP, Mahmoudi M, Devereux RB, Forrestal BJ, Mandawat A, Lyon AR, Chen CL, Barac A, Hung J, Thavendiranathan P, Picard MH, Thuny F, Ederhy S, Fradley MG, Neilan TG. Global Longitudinal Strain and Cardiac Events in Patients With Immune Checkpoint Inhibitor-Related Myocarditis. J Am Coll Cardiol 2020;75:467 – 78.
40. Pollack A, Kontorovich AR, Fuster V, Dec GW. Viral myocarditis–diagnosis, treatment options, and current controversies. Nat Rev Cardiol 2015;12:670–80.

Figures

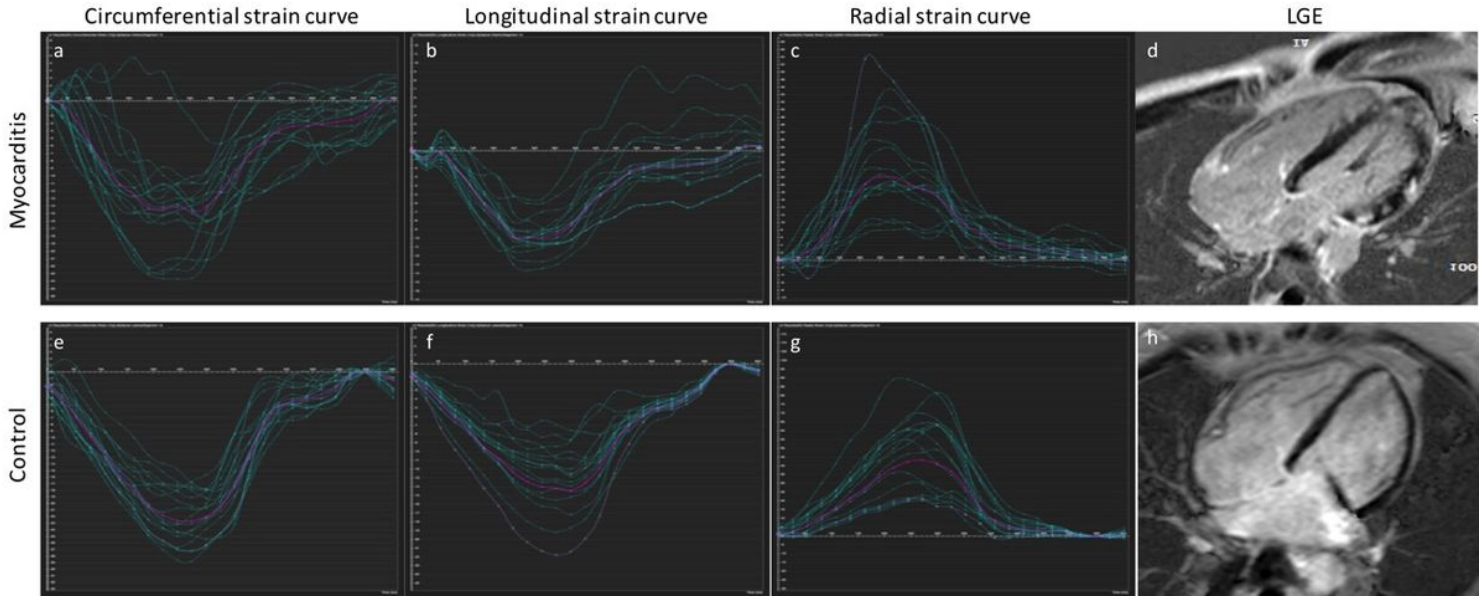

Figure 1

Circumferential strain curves, longitudinal strain curves, radial strain curves, and late gadolinium enhancement images (four-chamber view) for a patient with acute myocarditis (a-d, 28-year-old male; ejection fraction, 69.4%) and a healthy control (e-h, 30-year-old female; ejection fraction; 68.6%). The strain graph shows the circumferential, longitudinal, and radial strain of each segment (blue curves) vs. global strain (pink curve). Average circumferential, longitudinal, and radial strain are clearly reduced in the patient with acute myocarditis (global peak circumferential strain: -21.32% vs.-14.74%; global peak longitudinal strain: -13.53% vs. -10.0%; global peak radial strain: 38.67% vs. 22.05%). On late gadolinium enhancement imaging, typical patchy epicardial and midmyocardial inflammatory/necrotic lesions are visible.

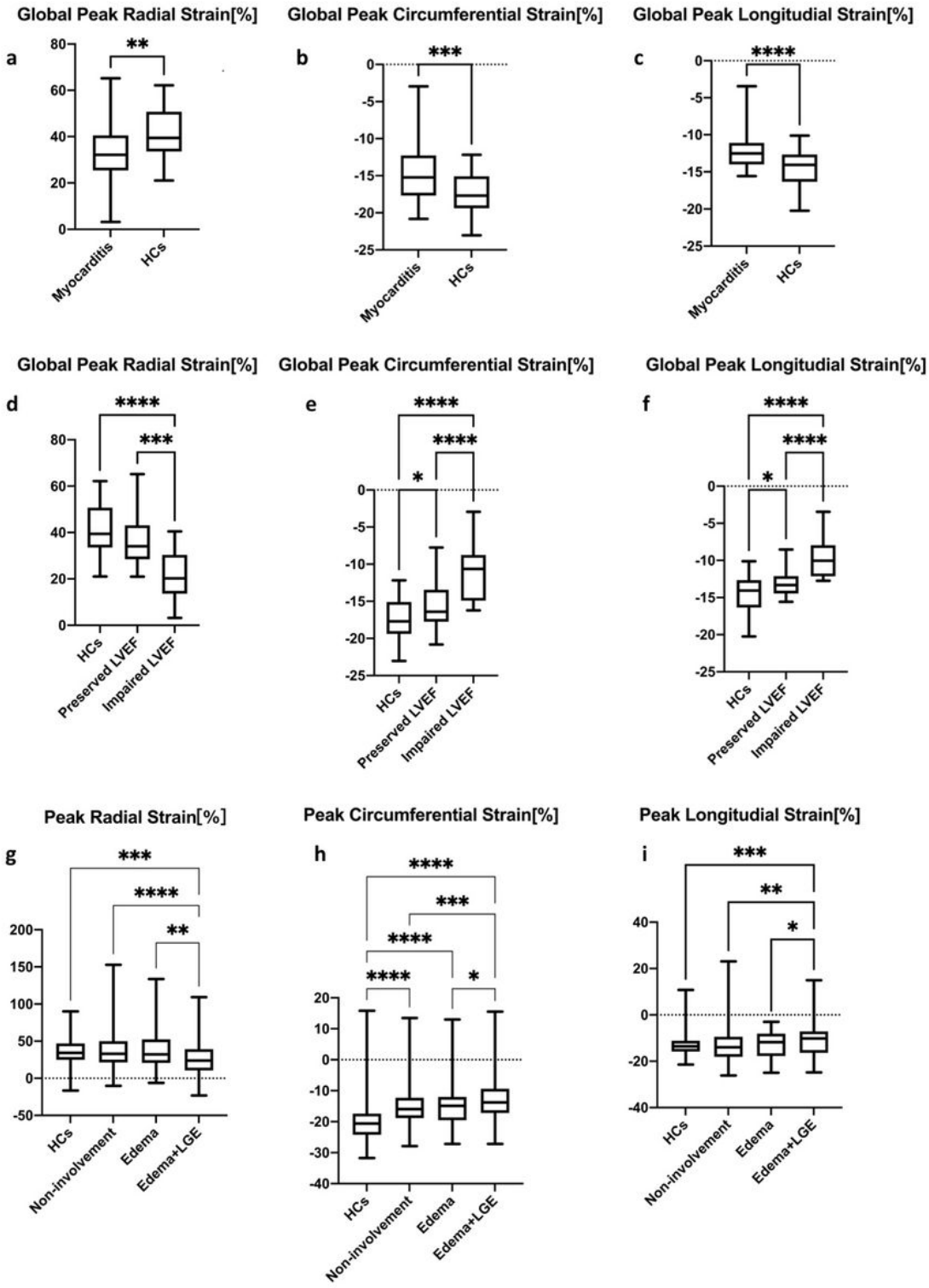

Figure 2

Comparison of global strain parameters between healthy controls and patients with suspected acute myocarditis(a-c). Comparison of global strain parameters between healthy controls, patients with preserved-LVEF and patients with impaired-LVEF(d-f). Comparison of segmental strain parameters between healthy controls, non-involvement segments, edema segments, edema and LGE segments(g-i).

*p<0.05; ** 0.001<p< 0.05; *** 0.0001<p< 0.001; **** p<0.0001

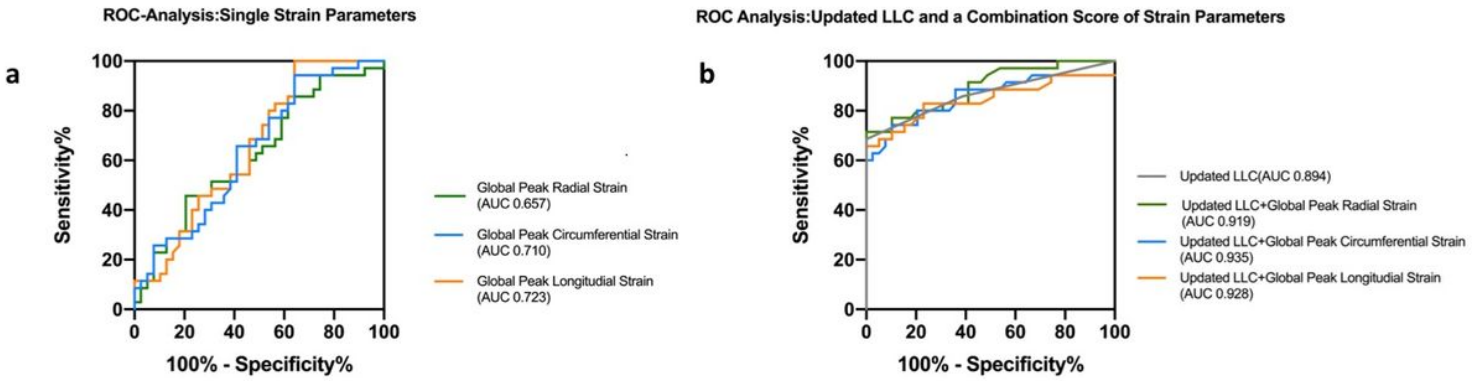

Figure 3

(a) Graph showing receiver operating characteristic curves for global peak longitudinal strain (area under the curve [AUC]: 0.723), global peak circumferential strain (AUC: 0.71), and global peak radial strain (AUC: 0.657). **(b)**Graph showing receiver operating characteristic curves for the updated Lake Louise Criteria (area under the curve [AUC]: 0.894) and for a combination score of global peak longitudinal strain (AUC: 0.928), global peak circumferential strain (AUC: 0.935), and global peak radial strain (AUC: 0.919).